NACA RM L55F13

NACA

RESEARCH MEMORANDUM

TESTS OF AERODYNAMICALLY HEATED MULTIWEB WING

STRUCTURES IN A FREE JET AT MACH NUMBER 2

TWO ALUMINUM-ALLOY MODELS OF 20-INCH CHORD

WITH 0.064- AND 0.081-INCH-THICK SKIN

By George E. Griffith, Georgene H. Miltonberger,
and Richard Rosecrans

Langley Aeronautical Laboratory
Langley Field, Va.

NATIONAL ADVISORY COMMITTEE
FOR AERONAUTICS

WASHINGTON

August 9, 1955

NACA RM L55F13 CONFIDENTIAL

NATIONAL ADVISORY COMMITTEE FOR AERONAUTICS

RESEARCH MEMORANDUM

TESTS OF AERODYNAMICALLY HEATED MULTIWEB WING

STRUCTURES IN A FREE JET AT MACH NUMBER 2

TWO ALUMINUM-ALLOY MODELS OF 20-INCH CHORD

WITH 0.064- AND 0.081-INCH-THICK SKIN

By George E. Griffith, Georgene H. Miltonberger,
and Richard Rosecrans

SUMMARY

Two 2024-T3 aluminum-alloy multiweb wing structures (MW-2 and MW-3), representative of airplane or missile wings, were tested at a Mach number of 2 under simulated supersonic flight conditions, and temperatures and strains were measured. The first model failed dynamically toward the end of its test because of the combined action of aerodynamic heating and loading. The second model, with thicker skin, survived tests up to an angle of attack of 3.5° but failed statically at an angle of attack of 5°. The model skin temperatures were in fair agreement with calculated values, but the stresses generally did not agree with expected results, possibly because of difficulty in converting the strain-gage data.

INTRODUCTION

As part of a program investigating the effects of aerodynamic heating on aircraft structures, the Structures Research Division of the Langley Laboratory is testing multiweb wing models under aerodynamic conditions similar to those encountered in supersonic flight at a Mach number of 2. The first structure MW-1, a multiweb wing of 40-inch chord and span, was tested primarily to obtain data on the temperature distribution, but the aerodynamic loads played an unanticipated role in that the model experienced a dynamic failure near the end of the test. Details of the test results and failure of model MW-1 are presented in reference 1, and the preliminary experimental results for the first seven models in the test program are given in reference 2.

CONFIDENTIAL

The second model MW-2, of 20-inch chord and span, was essentially a half-scale version of model MW-1 and was tested to compare its behavior with that of its prototype and to obtain additional information through increased instrumentation. This model also experienced a dynamic failure near the end of its test. The third model MW-3 was similar in size to model MW-2 but was provided with a thicker skin in order to withstand greater stresses, due to both loading and heating; this model failed statically at an angle of attack of 5° after surviving four tests at smaller angles of attack. The present paper discusses in detail the test results of models MW-2 and MW-3.

SYMBOLS

c specific heat, Btu/(lb)(°F)

h heat-transfer coefficient, Btu/(sq ft)(sec)(°F)

H stagnation pressure, lb/sq in. abs

t time from start of air flow, sec

t_0 time of initial conditions in temperature calculations, sec

T model temperature, °F

T_{AW} adiabatic wall temperature, °F

T_0 initial model temperature, °F

T_S stagnation temperature, °F

w specific weight, lb/cu ft

α angle of attack, deg

τ skin thickness, ft

TESTS

Models

The models designated MW-2 and MW-3 were identical in construction except for skin thickness; they comprised somewhat idealized semispan

cantilever multiweb wings with 5-percent-thick, symmetrical, circular-
arc airfoil sections (fig. 1). Model MW-2 had 0.064-inch-thick skin and
model MW-3 0.081-inch-thick skin. All material was 2024-T3 (24S-T3) alu-
minum alloy except that the rivets were either 2117-T (A17S-T) aluminum
alloy or Huck rivets and steel screws were used to attach the skins to.
the upper bulkhead. The surfaces of the models were sanded to provide
a finish of approximately 15 microinches, root mean square, and were
unpainted. Pertinent dimensions and details of construction of the
models are given in figure 1.

During a test a flat plate or fence surrounded the model approxi-
mately $19\frac{7}{8}$ inches below the model tip so that the fence projected
1/8 inch above the lower jet boundary and concealed the doubler plates,
lower bulkhead, and supporting structure from the airstream.

Instrumentation

Each model was instrumented with 24 iron-constantan thermocouples,
4 pressure orifices, and 24 Baldwin SR-4 type AB-11 wire strain gages.
(See fig. 2.) Locations were identical except that the strain gages
attached to model MW-2 at the station 11 inches from the model tip were
alined in the chordwise direction, whereas the gages at these locations
on model MW-3 were alined in the spanwise direction, and, in addition,
the forward pressure orifices for model MW-3 were located $3\frac{1}{4}$ inches from
the leading edge. Some instrumentation was inoperative at test time.
(For details concerning the installation and accuracy of the instrumen-
taion see the appendix.) Supplementary data were supplied through three
16-millimeter motion-picture cameras which operated at from about 75
to 230 frames per second.

Description of Tests

The tests were made at the Langley Pilotless Aircraft Research
Station, Wallops Island, Va., in the preflight jet, a blowdown wind tun-
nel in which models are tested in a free jet at the exit of a supersonic
nozzle. (See the appendix for additional details.)

Six test runs were made on the two models at a Mach number of 1.99
and at a stagnation pressure of approximately 120 lb/sq in. abs. All were
hot runs, $T_S \geq 432^\circ$ F, except for one cold run, $T_S = 98^\circ$ F, made on
model MW-3. For all test runs the stagnation pressure was attained in
2 seconds or less after air began to flow from the nozzle and then fluc-
tuated about the desired value until about 9 seconds (two tests) or 11 sec-
onds (three tests), with the exception that for run 5 on model MW-3 the

control valve was closed soon after the model had failed. Test time is reckoned from the time air began to flow out of the nozzle, and test conditions are considered to exist whenever the stagnation pressure exceeds 100 lb/sq in. abs. The stagnation temperatures approached test values almost immediately after the opening of the jet control valve. Detailed test conditions are given in table I and are discussed more fully under the section entitled "Test Facility" (see the appendix).

Model MW-2.- Model MW-2 was mounted vertically in the jet (root downward) at an angle of attack of 0.2° with its leading edge 2 inches downstream of the nozzle-exit plane (figs. 2 and 3). The model extended 20 inches into the airstream so that both the top of the doubler plates and the top of the fence (figs. 1 and 2) were about 1/8 inch above the lower jet boundary. After surviving the initial disturbance of the jet (see the appendix) the model remained steady until approximately 10 seconds at which time a vibratory motion took place; test conditions ended shortly thereafter (10.8 seconds) and during the shutdown phase of the jet the model experienced a partial failure.

Model MW-3.- Model MW-3 was located similarly to model MW-2 except that, as the tests progressed, the model was rotated in a counterclockwise fashion (looking at the top of the model) about a point $1\frac{1}{2}$ inches downstream of the trailing edge at successive angles of attack of -0.1°, -0.1°, 1.8°, 3.5°, and 5.0°. The first test was a cold run $\left(T_S = 98° F\right)$; the four remaining tests were hot runs. (For pertinent aerodynamic data, see table I.) Except for the temporary vibrations due to the starting and stopping phases of the jet, the model remained steady and survived runs 1 to 4 without sign of difficulty. At an angle of attack of 5° the model failed statically in bending at the root section just as test conditions were reached.

The two tests during which the models failed are described more fully in the section entitled "Model Failures."

RESULTS AND DISCUSSION

Experimentally Determined Test Conditions

Stagnation pressure.- Variations of the stagnation pressures with time for all test runs are given in figure 4. Fluctuations of these pressures during the tests indicate that test conditions (assumed to exist whenever $H \geq 100$ lb/sq in. abs.) were almost but never fully stabilized. The values reported in table I are average stagnation pressures during test conditions, except that for run 5 on model MW-3 the stagnation pressure is that obtained at the time of failure.

Stagnation temperature.- The stagnation temperature was obtained by averaging during the time of test conditions the average temperature of the two probes located just aft of the models (fig. 3). (This method is somewhat different from that used to obtain the stagnation temperature for the test on model MW-1; a short discussion of the reasons for so doing appears in the appendix.) Variations of the average probe temperature with time are given in figure 5. In these plots the apparent delay of approximately 0.7 second in reaching test conditions is due to time lag (see the section "Accuracy" in the appendix). The peak values shown in the plots at approximately 1 second are believed due to the stagnant mass of air in the heat accumulator; this air is somewhat hotter than that which follows it out of the jet when the control valve is opened.

Angle of attack.- The angle of attack for a given test was determined by using the experimental pressure differences at both pressure stations, slopes found from measured model ordinates, and second-order, small-perturbation theory, with the results at the rearward station being modified for tip effects in accord with the method of reference 3. Slightly different angles of attack were obtained at the two pressure stations. The values given in table I are the mean values for the two stations of the arithmetic test-run averages obtained during the time test conditions existed, except that for run 5 on model MW-3 the conditions used were those at the time of failure.

Model Temperatures

Model MW-2.- Only 14 of the 25 thermocouples attached to model MW-2 were in working order during the one test run on the model; temperatures were recorded for the five center skin panels and the first three webs and are given in table II in increments of 1 second until readings became erratic. As expected, the skin temperatures decreased slightly across the model chordwise, from front to rear. A spanwise decrease, from tip to root, was also indicated in that the temperatures recorded by thermocouples 5 and 6 were somewhat lower than other skin temperatures near the same chordwise station. The lower temperatures of thermocouples 5 and 6 may be partly due to some sink effect created by cementing lead wires to the under side of the skin, but are probably due more to the effect of the paraboliclike stagnation-temperature profile (see the appendix). During the test the interior temperatures lagged considerably behind the skin temperatures, but all temperatures were still increasing at a substantial rate at the end of the test; these results indicate that the test was transient in nature and of insufficient length to produce a steady-state temperature condition.

Plotted in figure 6 are some experimentally obtained temperatures which illustrate the effects of heat conduction from the skin to the interior of the model. The skin near the web (thermocouple 13) loses

heat to the interior and consequently has a somewhat lower temperature than the skin uninfluenced by heat conduction (thermocouples 10 and 11 — the average temperature of these two thermocouples has been plotted, since the individual temperatures differ by only a few degrees). For a point at the midheight of a web (thermocouple 21), heat is first conducted along the skin and then down into the web; hence, there is appreciable lag between the temperature at this point and the adjacent skin temperatures — the same is true for thermocouples 19 and 20 (not shown).

Model MW-3.- Nineteen or 20 of the 25 attached thermocouples were in working order for all test runs on model MW-3 and temperatures for these thermocouples for runs 2, 3, and 4 are given in table III. Run 1 was a cold test during which the model experienced measured increases in temperature ranging from 5° to 19° F, with the temperatures decreasing from leading to trailing edge and from tip to root, as for model MW-2. The highest temperature recorded was that for thermocouple 24 located in the solid leading-edge section. ·

For test runs 2, 3, and 4 (hot runs at angles of attack of -0.1°, 1.8°, and 3.5°) sample skin and web temperatures are shown in figure 6. The increase in skin thickness (from 0.064 inch for model MW-2 to 0.081 inch for model MW-3) should result in lower skin temperatures (for the same stagnation temperature), but in more heat being conducted into the interior than for model MW-2; hence the temperature differences between skin and web were not so great as for model MW-2 with its thinner skin. As was expected, for runs 3 and 4 (angles of attack of 1.8° and 3.5°) thermocouple 10 on the under side of the model experienced a faster temperature rise than thermocouple 11 (on the upper side). Again, the plots illustrate that steady-state conditions were not reached in the tests.

The fifth test run on model MW-3 (angle of attack of 5.0°) resulted in failure of the model just as test conditions were reached, and hence no temperature data are tabulated for this test; the measured temperatures had increased by approximately 20° to 70° F by the time of failure.

Skin temperatures (calculation A).- Comparisons between calculated and experimental skin temperatures are shown in figure 7 for only the skin locations corresponding to thermocouples 10 and 11. In the calculations the effects of conduction, radiation, and temperature variation through the skin thickness were considered negligible. The equation giving the temperatures is

$$T = T_{AW} - (T_{AW} - T_0)e^{-\frac{h(t-t_0)}{cw\tau}}$$

where T_0 is the initial temperature and t_0 is an initial time adjusted to allow for the variation in test conditions during the starting phase of the jet. Local flow conditions were used in the turbulent-flow formulas given in reference 4 to obtain the heat-transfer coefficient h and the adiabatic wall temperature T_{AW}.

Fairly good agreement between the calculated and test temperatures is evidenced in figure 7 for the tests on model MW-2 and model MW-3 run 2. In these plots the test values are the averages of thermocouples 10 and 11. For model MW-3 runs 3 and 4 (fig. 7), wherein the model was subjected to angles of attack of $1.8°$ and $3.5°$, the agreement is not very good, particularly so for the latter test. The differences in the temperatures of the two skins are about the same as the differences obtained from the calculations, but the magnitudes of the temperatures show poor agreement. This poor agreement could be due in part to some error in the test stagnation temperatures used in establishing h and T_{AW}, or possibly to some effect of angle of attack not considered in calculating h and T_{AW}, or to some error in the measured temperatures due to weakening of the bond between the thermocouple and the metal brought about by vibrations associated with repeated testing.

The results shown in figure 7 are representative of the overall agreement between calculated and test temperatures for all skin locations uninfluenced by heat conduction to other parts of the models.

Temperature distributions (calculation B).- Temperature histories for the complete chordwise cross sections of the models, corresponding to the test on model MW-2 and to test run 2 on model MW-3, were calculated by using a numerical procedure similar to that of reference 5. The model cross sections were each divided into eight segments of two types, one for the leading or trailing edge (plus adjacent skin) and the other for any skin and web combination (see, for example, ref. 6). The dividing lines between segments were chosen such that at these points heat conduction along the skin could be considered negligible. The segments for the solid leading or trailing edges and attached skin were then subdivided into 11 elements and any skin and web combination into 12 elements, as shown in figure 8. Values of the heat-transfer coefficient and adiabatic wall temperature obtained using local flow conditions and the turbulent-flow formulas of reference 4 were used in the calculations. No attempt was made to evaluate joint effects. The results, in the form of chordwise temperature distributions at both 3 and 8 seconds for the skin temperatures and the temperatures at the center line of the solid leading and trailing edges and of the webs, are presented in figures 9 and 10 with the corresponding experimental values. In addition, a few calculated temperature histories are compared with test values in figure 11.

Figures 9 and 10 show that the overall agreement between calculated and experimental values is fairly good for the skin temperatures of model MW-2 and both the skin and interior temperatures for run 2 on model MW-3. However, the calculations considerably overestimate the web temperatures for model MW-2. Part of this discrepancy may be due to resistance to the conduction of heat across the joint between skin and web not accounted for in the calculations. Comparison of a few calculated and experimental temperature histories given in figure 11 again illustrates that the agreement is generally fair except that the values for the web temperatures of model MW-2 are in poor agreement.

Strain-Gage Results

The models were instrumented with Baldwin SR-4 type AB-11 wire strain gages (see the section "Model Instrumentation" in the appendix) in order to obtain data on the distribution and magnitude of the stresses, both static and dynamic, and the frequency of any vibratory stresses. These gages were considered adequate for depicting vibrations, but since the gages were used under conditions for which they were not intended, the results in regard to stresses cannot be considered reliable and consequently are not plotted or tabulated.

It is believed that the gages yielded reliable information concerning the frequency and phasing of any vibratory stresses. All frequencies reported were obtained from the strain-gage records. Although the amplitudes of any vibratory stresses were damped considerably beyond 60 cycles per second (at 220 cycles per second the relative amplitude was about 0.2 true amplitude), the relative amplitudes, together with the phasing and frequencies, were helpful in reconstructing model behavior and in substantiating events seen in the motion pictures.

The tests subjected the models to two sources of stress, aerodynamic loading and aerodynamic heating, but by far the greater portion of stress at most strain-gage locations could be expected to be caused by aerodynamic heating. Such heating results in nonuniform temperature distributions across the chord (see, for example, figs. 9 and 10) and in the spanwise direction (see the preceding section "Model Temperatures"). These nonuniform temperature distributions produce uneven thermal expansion and therefore thermal stresses, principally compression in the skin in both the spanwise and chordwise directions. The test results indicate that substantial stresses apparently developed during all tests wherein the models were subjected to aerodynamic heating, but that very small stresses (less than 2 ksi in all but one case) resulted during the cold run (run 1 on model MW-3) when the temperatures changed insignificantly (19° F or less). Some approximate stress calculations, using the experimental temperature differences, indicate that the chordwise stress for model MW-2 was of the same order of magnitude as the critical buckling

stress. Although no stress analysis is presented herein for either model, reference 7 presents several methods, incorporating various degrees of approximation, for finding stresses and stress distributions resulting from thermal differences.

The preliminary results of reference 2, concerning the test on model MW-2 and the results for the chordwise skin strain gages across the chord 11 inches from the tip, were in substantial agreement with the expected results expressed in the preceding paragraph and approximate stress calculations. It was stated in reference 2 that "Approximate calculations and the recorded strains indicated that these two types of stresses were of about the same order of magnitude, around 6000 psi" (compression). At that time only preliminary calibration data were available, and data obtained between 80° F and 300° F were extrapolated to gage temperatures beyond 300° F where necessary in order to convert the strains to stresses. Later, more extensive calibration data revealed marked differences in gage behavior above 300° F. The results discussed herein were obtained using the later calibration data and show that the results of the test on model MW-2 are in marked disagreement with the statement in reference 2 and with the expected results, in that tensile stresses are almost universally indicated for these chordwise skin strain gages. For model MW-3 the skin strain gages at this chordwise station were alined in the spanwise direction, but, again, the gages were expected to be in compression. Once more the results were somewhat unexpected in that, with very few exceptions, the gages indicated tensile stresses. Although surprising, the results may merely reflect the effects of various inaccuracies upon the data reduction.

The gages mounted spanwise on the skin at the chordwise station $16\frac{1}{2}$ inches from the tip show moderately small stresses which increased with increased angle of attack, with the gages on the left skin (looking upstream) being in compression and the gages on the right side being in tension in accord with the aerodynamic forces. The temperatures for the skin gages at this station were somewhat lower than for the skin gages at the station 11 inches from the tip due to the sink effect of the webs and to the lesser stagnation temperature at this spanwise station. Thus the thermal stresses were not so great and the results were less affected by data-reduction inaccuracies (zero shift, etc.). Gages mounted on the webs always indicated tension, as expected, since the webs were cooler than the outer surface and provided restraint against the thermal expansion of the skin. Since these gages underwent the least temperature increases of any model gages, the data reduction was the least affected and the stresses, therefore, are probably the most reliable obtained. Results similar to those discussed in this and the preceding paragraph were found for run 5 on model MW-3 at the time of failure.

Model Failures

Model MW-2.- After experiencing some random vibrations due to the characteristic initial disturbance of the jet (see the appendix), model MW-2 remained steady until 9.8 seconds. At this time, as indicated by the motion pictures taken by cameras placed above the model and by the frequency, phasing, and amplitudes of the skin strain gages across the chord 11 inches from the tip, the model began to flutter at 226 cycles per second in a mode with about $1\frac{1}{2}$ waves along the chord and with the maximum amplitude near the trailing edge — a flag-waving action involving chordwise bending of the airfoil section that has been called chordwise flutter (refs. 2 and 8). Motion pictures taken from opposite sides of the model indicated that at approximately the same time, 10.0 seconds, a buckle had developed in the rearmost panel of both skins. At 10.8 seconds the stagnation pressure dropped below 100 lb/sq in. abs and test conditions were considered as having ended at this time. Shortly thereafter, at 11.5 seconds, and with the model still fluttering, the motion pictures showed the initial signs of failure to be a fracture of the tip rib and tearing of the adjacent skins just forward of the trailing edge. The piece of the tip rib tore away and was followed by tearing away of pieces of skin and the top part of the solid trailing-edge member. This was followed by further tearing of both skins in the next-to-last bay from the top of the model to about midsemispan, tearing away of an additional piece of skin and the trailing-edge member, and finally by the departure of the upper half of the next-to-last web. This last action occurred at 13.5 seconds by which time the entire upper rear corner had torn away. From about 13.5 to 14.2 seconds the model experienced additional disturbances associated with the shutdown characteristics of the jet. The failing action just described is illustrated in figure 12 by six frames taken from the motion pictures, and the model after the test is shown in figure 13.

If the jet had continued to run the model undoubtedly would have been completely destroyed as was model MW-1 (ref. 1).

The primary cause of failure was the aerodynamic heating since the model survived the starting disturbances without damage and then remained steady until the induced thermal stresses reduced the effective stiffness of the model (ref. 9) and caused it to flutter. At approximately the same time that the model began to vibrate, chordwise buckling of the skin developed in the rearmost bay; however, the exact order of flutter and skin buckling cannot be stated with certainty. The flutter could have been caused directly by thermal stresses which were insufficient to produce buckling but which were nevertheless sufficient to reduce the effective stiffness of the model to a point where flutter occurred, or the thermal stresses could have caused skin buckling (also a reduction in stiffness) which triggered off the model flutter. In either event the primary cause of failure was the aerodynamic heating. The flutter that

occurred (at 226 cycles per second) had about $1\frac{1}{2}$ waves along the chord with the maximum amplitudes at the trailing edge, a flag-waving action involving chordwise bending of the airfoil section and referred to as chordwise flutter; the distortions were somewhat similar to those shown in figure 6 of reference 2. (This type of flutter apparently has been little observed but is discussed to some extent in ref. 8.) Shortly after the model began to flutter, a fatigue failure of the tip bulkhead occurred in the form of tearing across the bulkhead at a section weakened by rivet holes. The adjacent skins (both sides) began to tear and the destruction continued as previously described. Since test conditions ended at 10.8 seconds and the bulkhead failure occurred at 11.5 seconds, all visible destruction actually took place during a period of decreasing stagnation pressure; had the jet continued to run, the model undoubtedly would have been completely destroyed. Motion pictures of the tests of models MW-2 and MW-3 can be obtained on loan from NACA Headquarters, Washington, D. C. (film entitled "Supersonic Jet Tests of Simplified Wing Structures").

Although the preliminary results of reference 2 indicated that the flutter of model MW-2 was induced by thermal buckling of the skin, the more extensive study of the motion pictures and the strain-gage records reported herein reveals that it is impossible to state positively the order in which these events occurred. The skin buckle in the rearmost bays (each side) developed gradually (and may also have been developing to a lesser extent in other bays), so that it is impossible to assign an exact time of buckling; hence, the time given (10.0 seconds) is that when an obvious buckle had developed. The wire strain-gage records reveal more definitely that at 9.8 seconds, approximately the time of skin buckling, the model began to flutter as already described.

Flutter associated with the aerodynamic heating of the models and the resulting thermal stresses is felt to be a function of the reduced stiffness of the structure brought about by a state of thermal stress which is dependent upon the nonuniformity of the temperature distribution but which is essentially independent of material property changes that are functions of the temperature level. (See, for example, ref. 9.) The only pertinent material property change that is expected to occur in the test time is in the modulus of elasticity, which would amount to a maximum reduction of about 10 percent. No known accurate criterion exists at present which will predict when and how structures such as these models will flutter.

The failures of model MW-2 and its larger scale original model MW-1 were fundamentally similar in that flutter, either accompanied by or closely preceded or followed by skin buckling, resulted in failure in the vicinity of the trailing edge. The primary cause of failure in both tests was aerodynamic heating. The thinner skin of model MW-2 caused its skin to become hotter faster than the skin of model MW-1, and the hotter skin and smaller webs of model MW-2 also resulted in higher interior

temperatures. Except for the tip bulkhead of model MW-2, which was within the airstream and underwent some temperature rise, the bulkheads of both models experienced negligible temperature changes. For both models the induced thermal stresses were insufficient to produce spanwise skin buckling but were, according to approximate calculations, sufficient to cause skin buckling in the chordwise direction. In the test of model MW-1, a vibratory motion began at 7.5 seconds accompanied by skin buckles which apparently originated in the skin panels near the leading edge; these buckles, appearing and disappearing rapidly, moved toward the trailing edge and settled there, whereas for model MW-2 the only appreciable buckles occurred at 10.0 seconds in the rearmost panels (both sides) — although the motion pictures indicated that perhaps smaller buckles might have been forming in other panels; in each case the buckling in a panel was a long, narrow chordwise skin buckle. Both models apparently experienced some kind of flutter, but whereas the flutter of model MW-2 has been described with some certainty, the fluttering action of model MW-1 cannot. In both cases, the most violent action occurred near the trailing edge and destruction began in this region. It is felt that the destruction of model MW-2 would have been as violent and complete as that of its predecessor had the air flow lasted only slightly longer.

Model MW-3.- Beginning at 0.2 second after the air began to flow through the jet, model MW-3 (at an angle of attack of 5°) vibrated, mainly in bending, at approximately 65 cycles per second until the initial normal shock reached the leading edge of the model. At this time, 1.0 second, the model steadied. The normal shock wave had moved to the model midchord at 1.2 seconds, then moved downstream and disappeared. The model continued to remain steady until 1.8 seconds, at which time test conditions had been reached and the aerodynamic forces had become sufficiently large to produce compressive buckling of the skin at the root section. At this time the model collapsed on its side to the position shown in figure 14.

The failure was almost entirely independent of any aerodynamic-heating effects, since the maximum measured temperature rise (70° F) was insufficient to produce any noticeable changes in the properties of the material and the temperature differences in the structure (approximately 35° F near the middle of the model) were so small that only negligible thermal stresses had developed. Thus the failure was almost solely due to aerodynamic loading. At the time of failure the aerodynamic forces had increased to slightly beyond the prescribed value (H = 106 lb/sq in. abs), and the calculated force of about 6.7 lb/sq in. (970 lb/sq ft) was sufficient to cause the skin to wrinkle completely across the chord and to crush the webs on the compression side of the model. As soon as the skin wrinkled the aerodynamic forces pushed the model completely over on its side.

CONCLUDING REMARKS

Six tests on two multiweb wing models were made under simulated aerodynamic conditions, and temperatures and strains were measured, with the following results:

For the five tests wherein the models experienced aerodynamic heating, the surface temperatures always exceeded the interior (web) temperatures. Skin temperatures were hottest near the leading edge and progressively cooler toward the trailing edge with corresponding dips near the heat sinks created by the webs. The highest recorded temperatures were those in the solid leading-edge member. For points in the skin midway between webs, the measured temperatures showed only fair agreement with calculated temperatures wherein heat conduction was considered negligible (calculation A), the agreement being progressively worse as the angle of attack increased. Detailed calculations of the complete chordwise cross-sectional temperature distributions for models MW-2 and MW-3 run 2 (calculation B) showed generally fair agreement with the experimental temperatures except that the interior temperatures for model MW-2 were considerably overestimated.

Much of the stress data disagrees with expected results, but so much uncertainty encompasses the reduction of the strain data that no conclusions can be made concerning the results. The strain data were useful, however, in providing phasing and frequency information and in helping to reconstruct model behavior.

Model MW-2 experienced a partial dynamic failure late in its test (just after the stagnation pressure began to diminish), apparently brought on by aerodynamic heating which caused a reduction in stiffness of the model, skin buckling, and flutter. The model would undoubtedly have been completely destroyed had the flow of air continued a short time longer.

The first test on model MW-3, a cold run, indicated that for the remaining tests, except for run 5 wherein the model failed, at least a substantial portion of most stresses obtained from the measured strains was the result of aerodynamic heating. The thicker skin of model MW-3 prevented the occurrence of flutter even when the model was tested at angles of attack of 1.8° and 3.5°. At an angle of attack of 5.0° the

aerodynamic forces were sufficient to cause the compressive skin to wrinkle and the model to fail statically.

Langley Aeronautical Laboratory,
    National Advisory Committee for Aeronautics,
        Langley Field, Va., May 23, 1955.

APPENDIX

APPARATUS, INSTRUMENTATION, AND ACCURACY

Test Facility

The preflight jet is a blowdown wind tunnel in which models are tested in a free jet at the exit of a supersonic nozzle. When a pressure control valve is opened, dry air escapes from two storage spheres and passes through a heat accumulator that can be preheated to provide stagnation temperatures up to 600° F. The control valve regulates the flow of air and maintains a free-stream pressure of about 1 atmosphere at the nozzle exit. For the Mach number 2, 27- by 27-inch nozzle used in these tests, stabilized aerodynamic conditions can be maintained at the exit of the nozzle for approximately 9 seconds after a starting period of 2 seconds. Three additional seconds are required to shut down the jet, so that the total test time is about 14 seconds.

Starting and shutdown characteristics of the jet.- At the beginning and end of a test, there occurs a twofold disturbance which is a characteristic of the test facility but independent of any aerodynamic heating. This disturbance, which temporarily affects the model, takes place whenever the stagnation pressure exceeds 16 lb/sq in. abs but is less than 105 lb/sq in. abs. When a test begins the first stage of this twofold disturbance occurs when the stagnation pressure is less than 50 lb/sq in. abs. During this time the normal shock is inside the nozzle, the flow over the model is subsonic and very turbulent, and the model undergoes severe random vibrations — mostly in bending but with some torsion. The second stage of the disturbance begins when the stagnation pressure reaches 50 lb/sq in. abs. At this time the flow over the leading edge of the model becomes supersonic, the violent model vibrations stop, and a complicated shock pattern develops over the model. This shock pattern, which originates at the nozzle, reduces to oblique shocks of negligible strength when the stagnation pressure reaches 105 lb/sq in. abs. During this second stage the pressure variations appear to have little effect on the model other than to tend to produce local skin deformation or bending.

At the close of a test these stages occur in reverse order.

Stagnation temperature.- The test of model MW-1 (ref. 1) revealed some difficulty in determining an accurate test stagnation temperature; for lack of a better method, the stagnation temperature for the test on model MW-1 was taken as the arithmetic average of temperatures from nine thermocouples mounted on a rake downstream of the heat accumulator, with the spread in individual values exceeding 100° F. For succeeding tests the rake temperatures were again recorded, but, in addition,

two stagnation-temperature probes were mounted just aft of the model,
where the temperature distribution was expected to be more uniform, and
at the approximate height of the main model thermocouple installation
(10 inches from the tip). Shortly after the tests on models MW-2
and MW-3, limited surveys were taken at the nozzle exit in order to
determine the stagnation-temperature distribution across the vertical
center line of the jet just downstream of the nozzle exit.

For the tests on models MW-2 and MW-3 the stagnation temperatures,
measured by either eight or nine thermocouples in the rake downstream of
the heat accumulator, varied by 110° F for the cold run (run 1 on
model MW-3) and by an average of 217° F for the hot runs (all remaining
tests except run 5 on model MW-3). The two stagnation-temperature probes,
located 23.5 inches from the nozzle exit and approximately at midheight
of the models, varied by 9° F for the cold run and an average of 28° F for
four hot runs (only one probe was in operation during run 2 on model MW-3).
In all cases the individual temperatures were nearly constant with time.
However, the average temperature of the rake thermocouples was not in
very good agreement with the average of the probe thermocouples; the dis-
agreement varied from 25° F to 56° F (not including run 5 on model MW-3).
The survey tests showed that the stagnation-temperature profile across a
vertical center line at the nozzle exit is roughly parabolic and that the
maximum temperature near the center exceeds the temperature at the edges
by approximately 100° F. During these tests a few temperatures were meas-
ured at the approximate height of the probe thermocouples and then com-
pared with the probe temperatures; in each case the agreement was fairly
good.

From the foregoing discussion it is evident that some uncertainty
accompanies the determination of an accurate test stagnation temperature.
However, since the probes were located in the stream near the models and
at the approximate height of most of the model instrumentation, an aver-
age of the probe temperatures was considered the most accurate indication
of the test conditions. These temperatures, averaged during test times,
are listed in table I. Plots of these stagnation temperatures are also
given in figure 5.

Model Instrumentation

Thermocouples.- Thermocouples were peened into small holes drilled
into the skin and webs; the skin thermocouples were located at the mid-
plane of the skin. In the leading- and trailing-edge sections, the thermo-
couples were covered with cement and then inserted in small holes drilled
into these solid sections.

Pressures.- The model pressure-pickup installation, used only to
determine the angle of attack, consisted of 0.059-inch-inside-diameter

copper tubing, approximately 18 inches in length, leading from an
0.059-inch-diameter orifice in the skin to a Statham pressure transducer
outside the model. Tubing from both skins was connected to pressure
transducers in such a manner that both pressure for the left side,
looking upstream, and differential pressure (right side) were obtained
at the two chordwise pressure stations shown in figure 2.

Strain gages.- Baldwin SR-4 type AB-11 wire strain gages were attached
to the models (at the locations shown in fig. 2) in accordance with the
manufacturer's specifications and cured to 250° F. The gages were then
cycled twice to 300° F by inserting the models in an oven and gradually
increasing the temperature from 80° F to 300° F in 2 hours, with the
temperature being maintained at 300° F for approximately 12 minutes,
allowing the models to cool, and repeating the process. During the sec-
ond cycle the zero shifts of the individual gages were measured. Although
model temperatures in excess of 300° F were anticipated, the curing tem-
peratures were not allowed to exceed 300° F in order to minimize changes
in the mechanical and physical properties of the 2024-T3 material. Since
these strain gages are non-temperature-compensating, calibration data were
obtained for sample gages cured in the same manner, but the calibration
data were necessarily obtained under steady-state conditions. The cali-
bration tests indicated that a marked difference in zero shift takes place
beyond 300° F (for gages which have never previously exceeded this tem-
perature). Moreover, this zero shift can be of the order of magnitude
of the indicated strain, varies from gage to gage, and is dependent upon
the gage temperature, which may not be accurately known. In addition to
the aforementioned factors there are others which adversely affect the
interpretation of the strain-gage results.

Accuracy

Listed below are the estimated probable errors in individual meas-
urements and also the corresponding time constants. The time constant,
which is considered independent of the probable error, is defined as the
time at which the recorded value for a step-function input is 63 percent
of the input; at three time constants the response amounts to 95 percent
of the input.

Item	Probable error	Time constant
Stagnation pressure	± 0.7 lb/sq in.	0.03 sec
Stagnation temperature	$\pm 3^\circ$ F	.12 sec
Model temperature	$\pm 3^\circ$ F	.03 sec
Model pressure	± 0.1 lb/sq in.	.03 sec
Model strain	± 80 μin./in.	.02 sec

Errors due to the thermocouple installation have not been included above, but they are probably small. The maximum temperature difference through the skin thickness was estimated to be less than 5° F, so that thermocouples in the skin should measure the average skin temperature within 2° F.

Calibration tests showed the Mach number to be 1.99 ± 0.02.

REFERENCES

1. Heldenfels, Richard R., Rosecrans, Richard, and Griffith, George E.: Test of an Aerodynamically Heated Multiweb Wing Structure (MW-1) in a Free Jet at Mach Number 2. NACA RM L53E27, 1953.

2. Heldenfels, Richard R., and Rosecrans, Richard: Preliminary Results of Supersonic-Jet Tests of Simplified Wing Structures. NACA RM L53E26a, 1953.

3. Czarnecki, K. R., and Mueller, James N.: An Approximate Method of Calculating Pressures in the Tip Region of a Rectangular Wing of Circular-Arc Section at Supersonic Speeds. NACA TN 2211, 1950.

4. Chauvin, Leo T., and DeMoraes, Carlos A.: Correlation of Supersonic Convective Heat-Transfer Coefficients From Measurements of the Skin Temperature of a Parabolic Body of Revolution (NACA RM-10). NACA RM L51A18, 1951.

5. Kaye, Joseph: The Transient Temperature Distribution in a Wing Flying at Supersonic Speeds. Jour. Aero. Sci., vol. 17, no. 12, Dec. 1950, pp. 787-807, 816.

6. Griffith, George E.: Transient Temperature Distribution in an Aerodynamically Heated Multiweb Wing. NACA RM L53E27a, 1953.

7. Heldenfels, Richard R.: The Effect of Nonuniform Temperature Distributions on the Stresses and Distortions of Stiffened-Shell Structures. NACA TN 2240, 1950.

8. Halfman, Robert L., and Ashley, Holt: Aeroelastic Properties of Slender Wings. Proc. First Nat. Cong. Appl. Mech. (Chicago, Ill., 1951), A.S.M.E., 1952, pp. 907-916.

9. Vosteen, Louis F., and Fuller, Kenneth E.: Behavior of a Cantilever Plate Under Rapid-Heating Conditions. NACA RM L55E20c, 1955.

TABLE I.- AERODYNAMIC TEST DATA

Test		Angle of attack, deg	Mach number	Stagnation pressure, lb/sq in. abs	Stagnation temperature, °F	Free-stream static pressure, lb/sq in. abs	Free-stream dynamic pressure, lb/sq in.	Free-stream temperature, °F	Free-stream velocity, fps	Free-stream density, slugs/cu ft	Speed of sound, fps	Reynolds number per foot
Model	Run											
MW-2	1	0.2	1.99	118	432	15.2	42.3	38	2.18×10^3	2.57×10^{-3}	1.10×10^3	15.4×10^6
MW-3	1	-.1	1.99	113	98	14.6	40.5	-149	1.72	3.94	.86	27.9
	2	-.1	1.99	120	451	15.5	43.0	48	2.20	2.56	1.10	15.3
	3	1.8	1.99	121	466	15.7	43.5	57	2.22	2.54	1.12	15.1
	4	3.5	1.99	119	475	15.4	42.7	62	2.23	2.47	1.12	14.6
	5	5.0	1.99	106	480	13.8	38.3	65	2.24	2.20	1.12	13.0

TABLE II.- TEMPERATURES FOR MODEL MW-2

t, sec	Temperature, °F, at thermocouple													
	5	6	9	10	11	13	14	15	16	17	19	20	21	22
0	87	88	88	89	89	90	91	87	88	87	89	89	89	88
1	118	116	132	124	127	122	126	119	117	118	92	93	88	100
2	164	166	179	177	181	165	172	171	167	164	107	96	92	129
3	209	213	231	226	233	209	217	219	211	203	142	108	102	171
4	245	247	274	266	273	246	252	257	246	235	183	130	118	208
5	273	275	307	297	305	278	283	288	277	262	223	155	137	241
6	294	295	333	321	329	302	307	312	301	286	257	179	154	269
7	312	311	355	340	348	322	327	331	321	305	286	202	173	294
8	325	324	371	356	363	339	344	347	337	321	309	225	196	314
9	336	334	384	367	374	351	355	359	347	332	328	240	215	330
10	---	338	403	---	387	353	---	378	362	---	---	259	242	341

TABLE III.- TEMPERATURES FOR MODEL MW-3

Run	t, sec	Temperature, °F, at thermocouple																			
		1	2	3	4	5	6	7	10	11	12	13	15	16	18	19	20	21	22	24	25
2	0	85	84	86	85	85	82	80	84	86	86	87		84	84	87	86	86	85	85	80
	1	116	113	109	118	110	114	105	113	113	116	112		111	109	91	90	86	100	96	89
	2	169	168	155	172	157	166	143	162	158	162	154		158	157	110	103	93	130	141	125
	3	224	227	204	226	205	216	183	210	204	209	199		201	190	152	134	108	169	197	163
	4	270	272	249	269	248	255	221	249	247	252	239		240	221	202	180	135	209	254	192
	5	305	309	283	303	279	286	244	286	281	285	272		272	248	249	217	164	245	299	222
	6	333	337	310	329	305	311	264	312	308	310	298		296	269	285	251	196	275	338	246
	7	353	360	331	350	324	332	277	333	328	333	319		319	289	318	283	229	301	367	267
	8	372	378	349	367	340	345	289	352	347	352	338		335	304	342	309	256	322	390	287
	9	386	392	363	381	353	357	297	366	361	365	354		351	319	363	331	282	341	406	305
	10	397	404	374	392	362	366	301	378	372	377	365		361	330	378	349	303	355	418	319
	11	406	413	384	401	370	374	307	388	382	386	375		372	340	390	364	319	367	427	330
	12	412	420	391	407	375	380	308	395	389	394	383		378	348	398	374	334	378	433	342
	13	417	424	395	412	378	385	309	400	394	398	389		384	360	405	383	345	385	438	354
	14	420	426	400	416	381	387	309	404	400	407	400		392	370	415	397	355	394	441	366
3	0	71	71	73	72	71	71	70	71	74	74	73	84	74	74	74	75	75	72	72	72
	1	104	94	97	104	100	102	97	98	100	106	102	102	103	99	79	80	76	89	83	80
	2	151	147	140	160	143	153	135	151	140	150	137	144	144	141	91	91	82	122	125	110
	3	204	207	187	210	188	202	177	200	185	196	181	183	184	173	124	123	100	158	183	148
	4	244	250	224	248	224	238	205	240	221	230	215	214	216	199	158	162	125	192	237	180
	5	277	281	254	279	255	265	229	270	252	262	245	238	245	222	193	199	153	222	279	207
	6	304	308	280	304	280	289	250	295	277	286	269	258	268	241	225	234	181	250	315	230
	7	324	328	299	324	299	307	263	315	297	306	289	275	287	259	258	263	208	272	342	251
	8	341	344	318	340	317	321	278	332	314	323	307	288	303	274	288	287	231	293	363	270
	9	354	358	332	354	330	335	285	345	325	337	320	301	317	287	313	308	250	309	379	284
	10	364	370	342	367	338	349	288	357	335	344	332	307	323	295	340	324	273	319	391	298
	11	373	377	349	373	343	353	289	364	343	352	342	319	335	310	353	338	289	330	399	314
	12	377	381	357	379	346	358	289	371	351	361	351	318	344	318	368	351	304	342	405	326
	13	377	382	358	381	347	359	288	371	351	360	350	318	343	318	375	359	317	346	406	329
	14	377	384	359	381	350	360	285	373	351	358	351	317	341	317	378	363	326	347	407	330
4	0	72	72	73	72	72	69	69	69	72	73	71		72	70	72	73	72	71	72	69
	1	105	90	99	101	100	97	95	94	96	105	99		102	98	78	77	74	88	82	78
	2	153	141	142	159	143	149	137	149	132	145	132		143	138	93	89	80	119	127	109
	3	200	202	186	204	188	188	180	192	169	183	168		178	167	128	121	99	152	182	148
	4	236	243	220	240	221	221	213	228	201	215	198		205	189	165	159	125	182	233	179
	5	265	272	248	267	251	246	234	249	230	242	225		231	210	201	196	154	210	275	206
	6	290	296	270	291	274	270	258	270	253	263	246		251	227	233	229	180	234	309	229
	7	310	315	292	310	294	287	276	287	272	283	266		269	244	262	257	207	256	333	247
	8	324	328	306	324	310	303	288	302	288	298	283		285	259	283	282	231	276	353	266
	9	339	341	321	337	324	316	300	315	301	312	296		297	272	303	302	251	291	365	280
	10	347	351	330	347	334	328	305	327	313	324	309		308	282	316	318	269	305	378	290
	11	355	359	338	357	342	341	311	339	322	332	320		316	291	325	330	286	315	386	304
	12	363	368	345	368	348	352	312	351	329	339	327		321	296	337	341	302	322	391	313
	13	368	374	352	373	352	357	313	356	339	348	336		330	311	347	347	308	334	395	324
	14	374	379	361	379	356	363	310	367	350	361	350		343	322	369	359	317	---	400	336

Figure 1.- Dimensions of multiweb wing models MW-2 and MW-3.

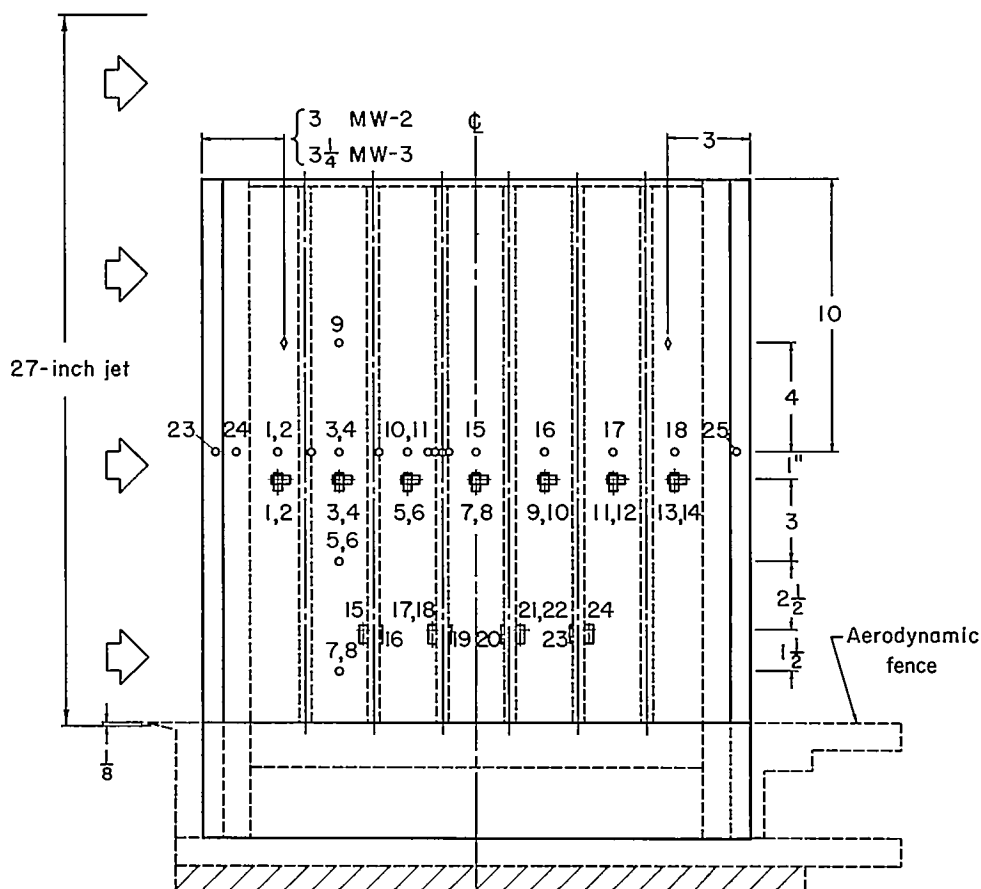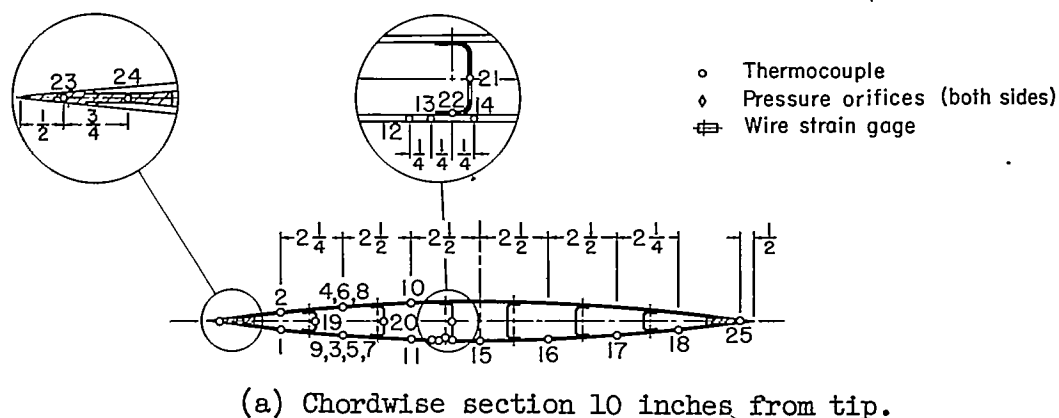(a) Chordwise section 10 inches from tip.

(b) Plan view.

Figure 2.- Location of instrumentation for models MW-2 and MW-3. (Where two wire strain gages are listed,.even-numbered gage is on far skin. Strain gages 16, 19, 20, and 23 are along web center line. The strain gages 11 inches from the tip are alined in the chordwise direction on model MW-2 and in the spanwise direction on model MW-3.)
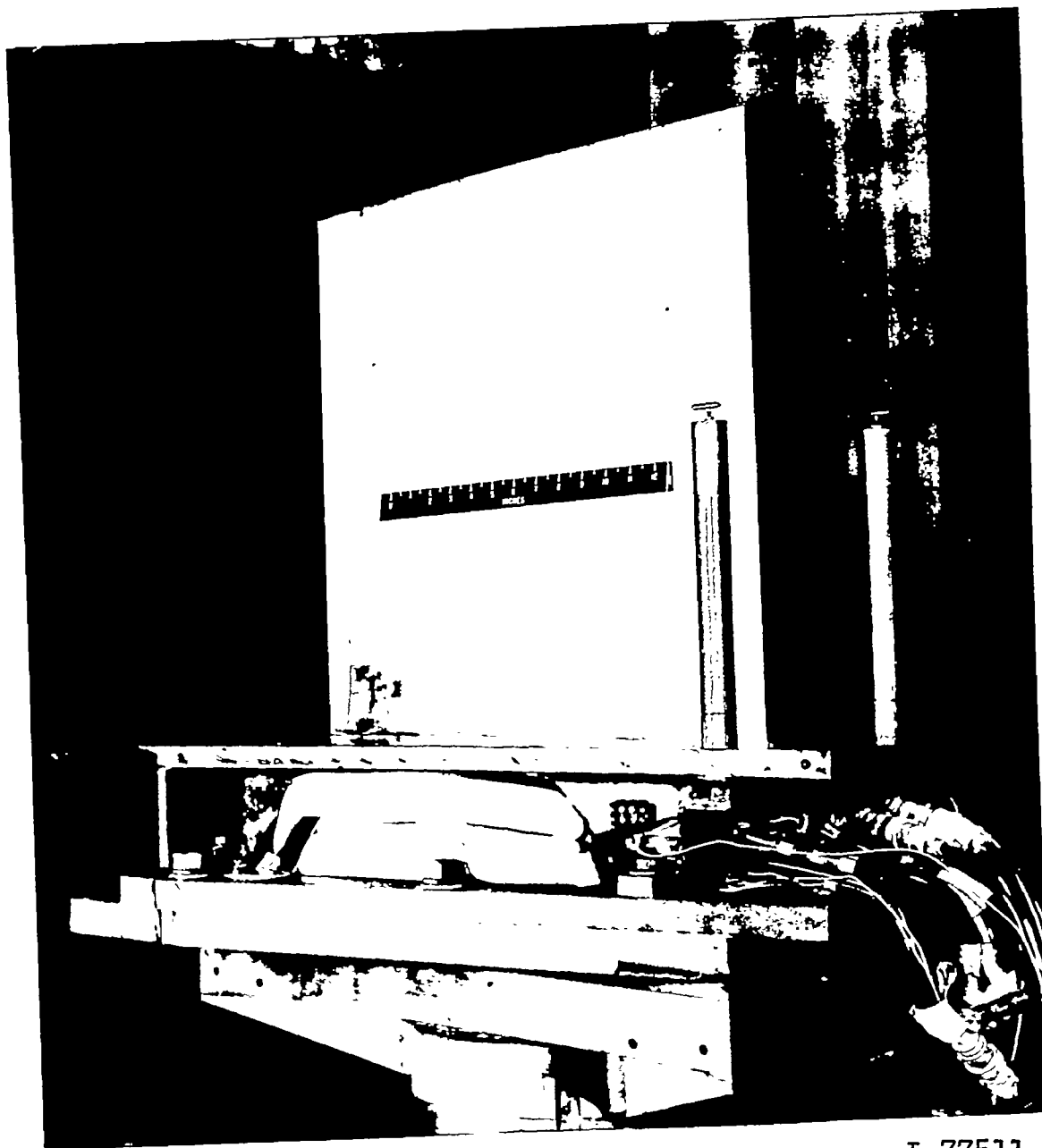
L-77511

Figure 3.- Model in place at nozzle exit prior to test. (Stagnation-temperature probes can be seen behind model.)
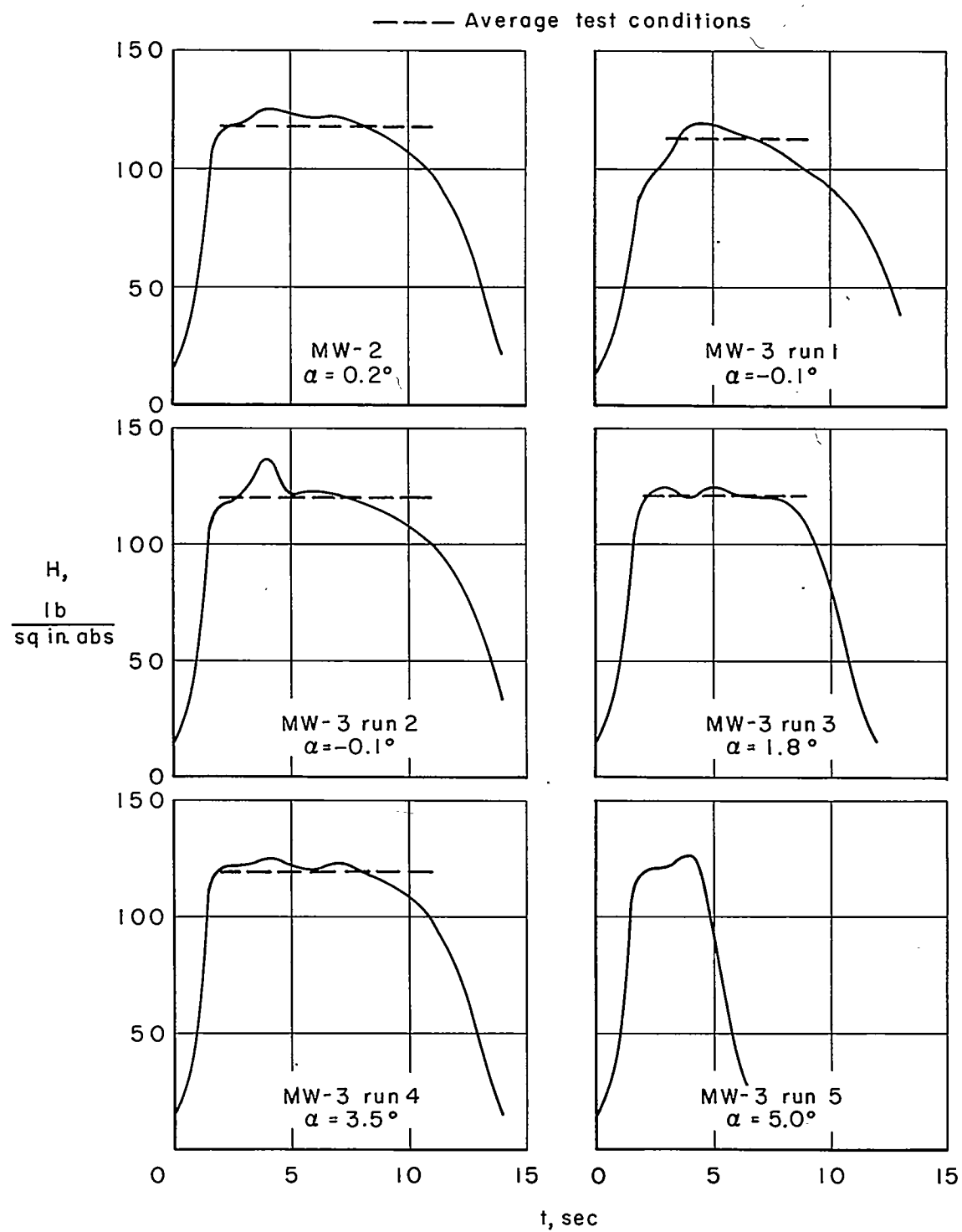
Figure 4.- Stagnation pressures.

CONFIDENTIAL   NACA RM L55F13
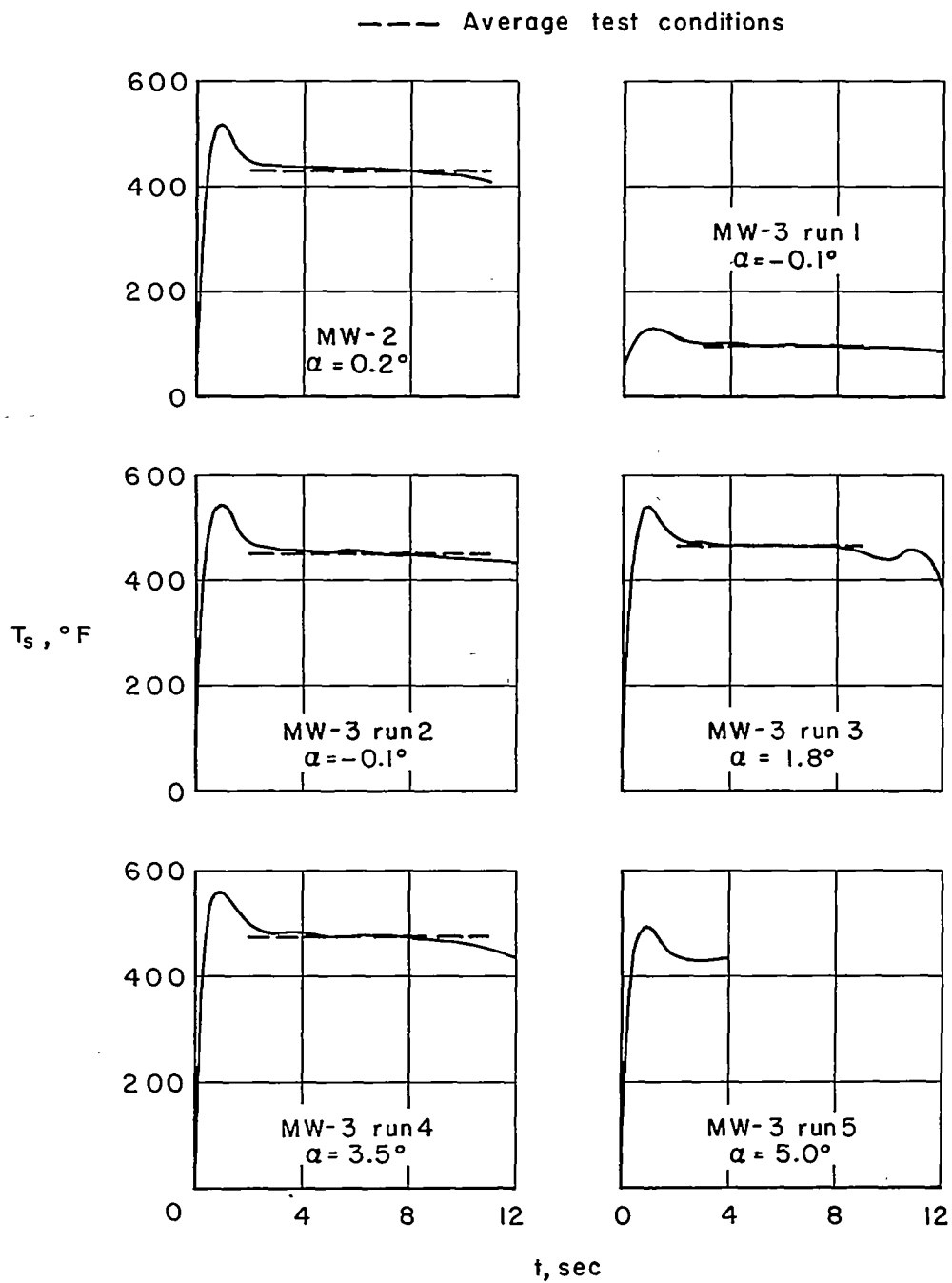
Figure 5.- Stagnation temperatures.
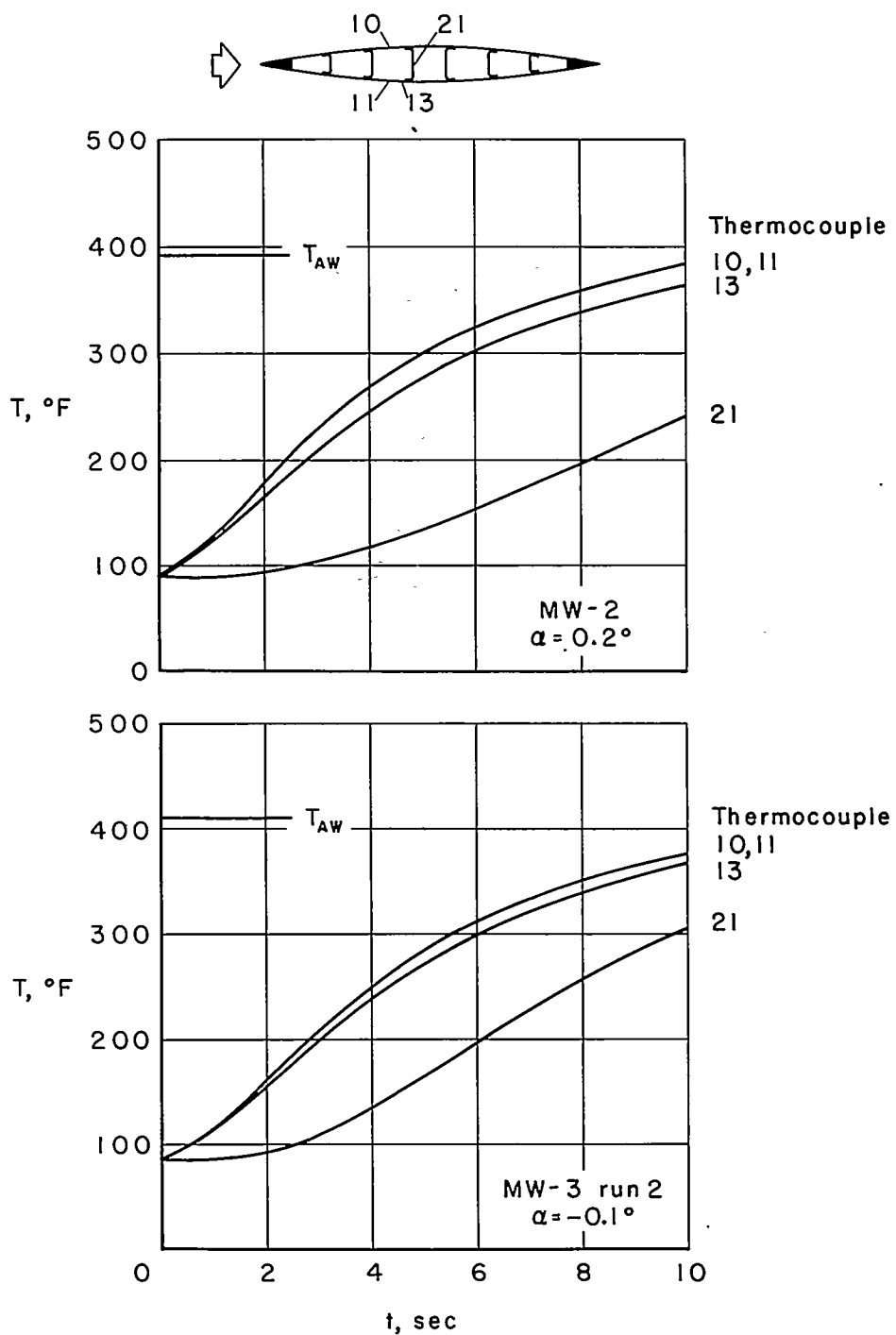
Figure 6.- Typical model temperatures.
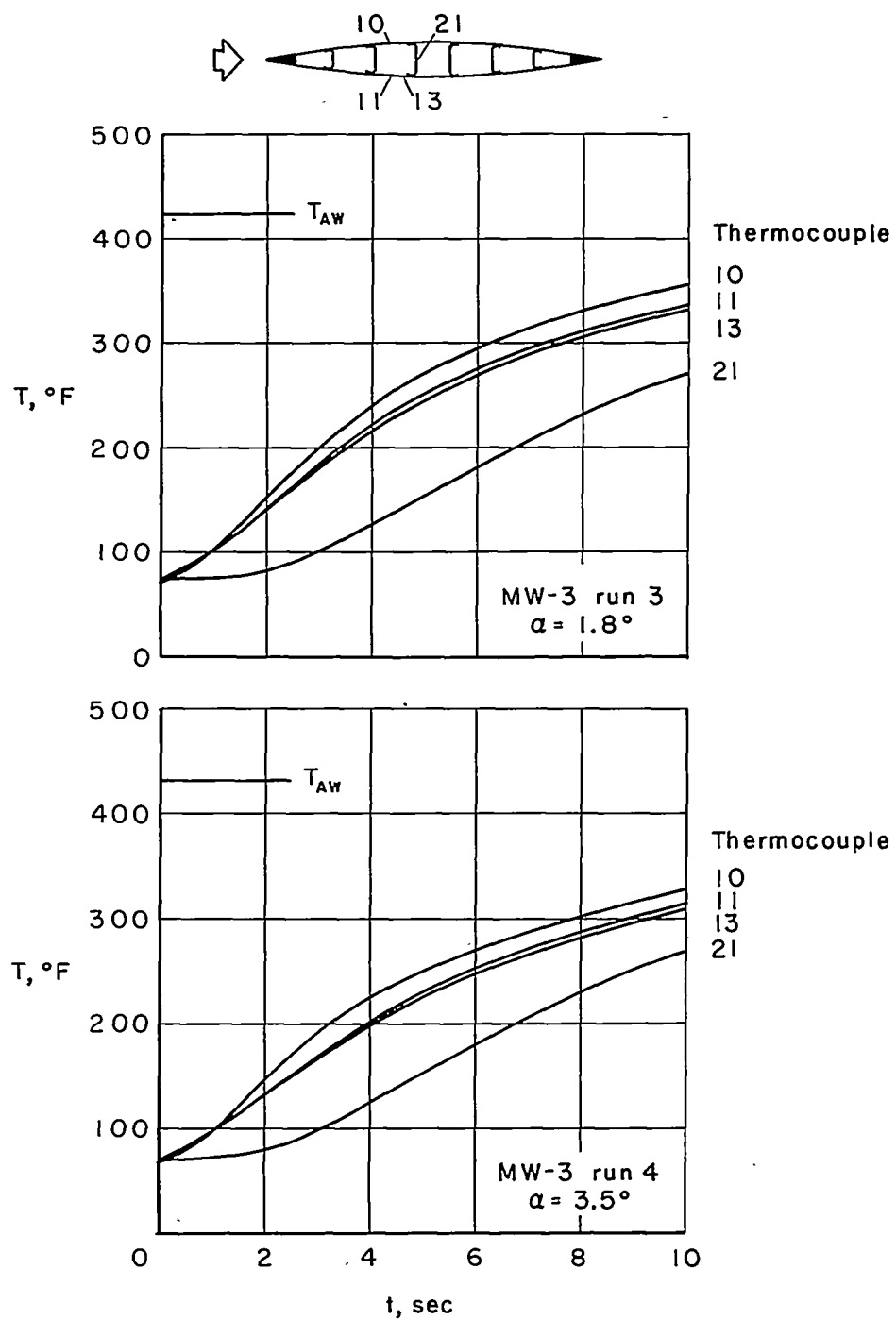
Figure 6.- Concluded.
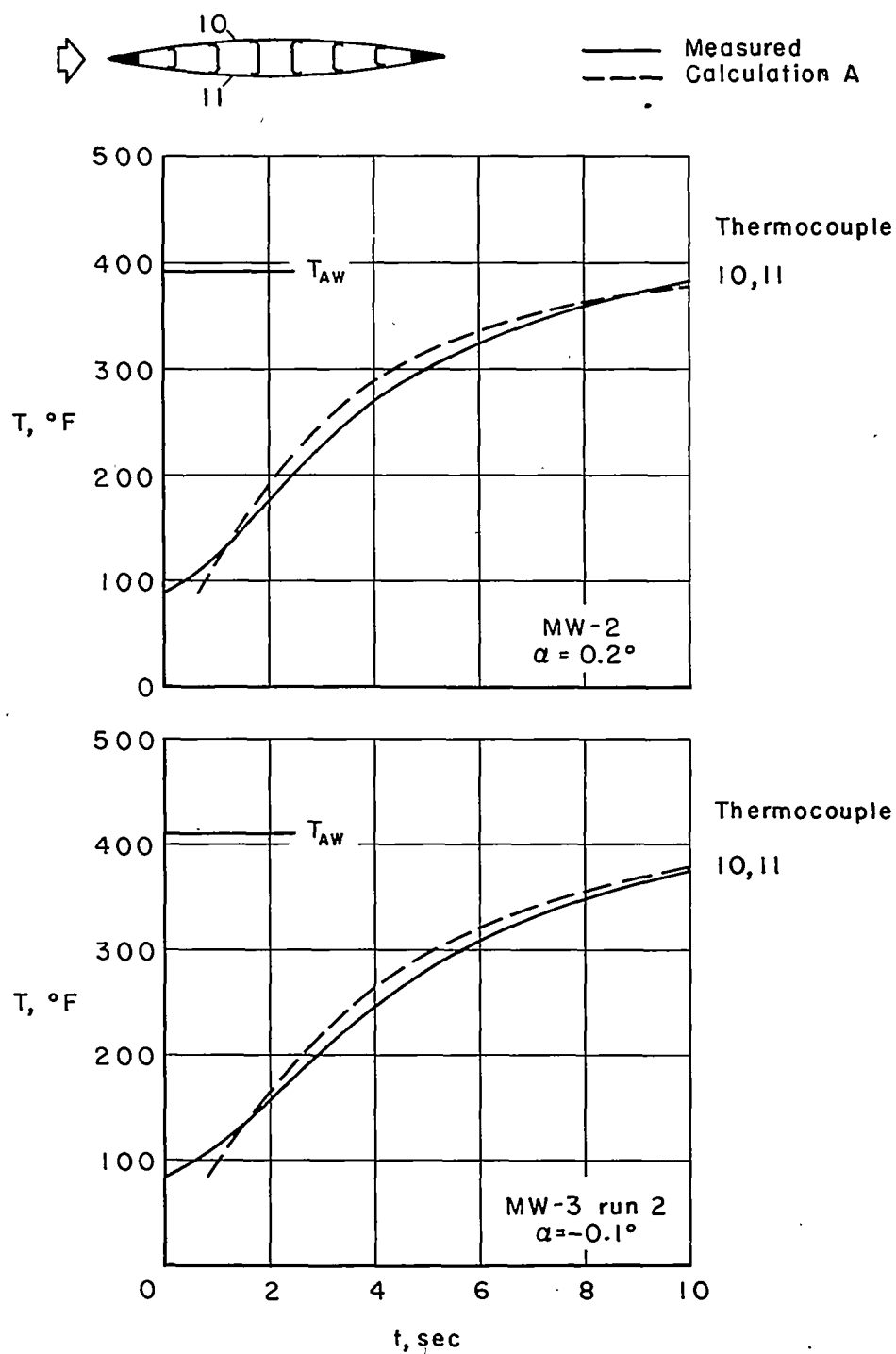
Figure 7.- Comparison of measured and calculated skin temperatures.
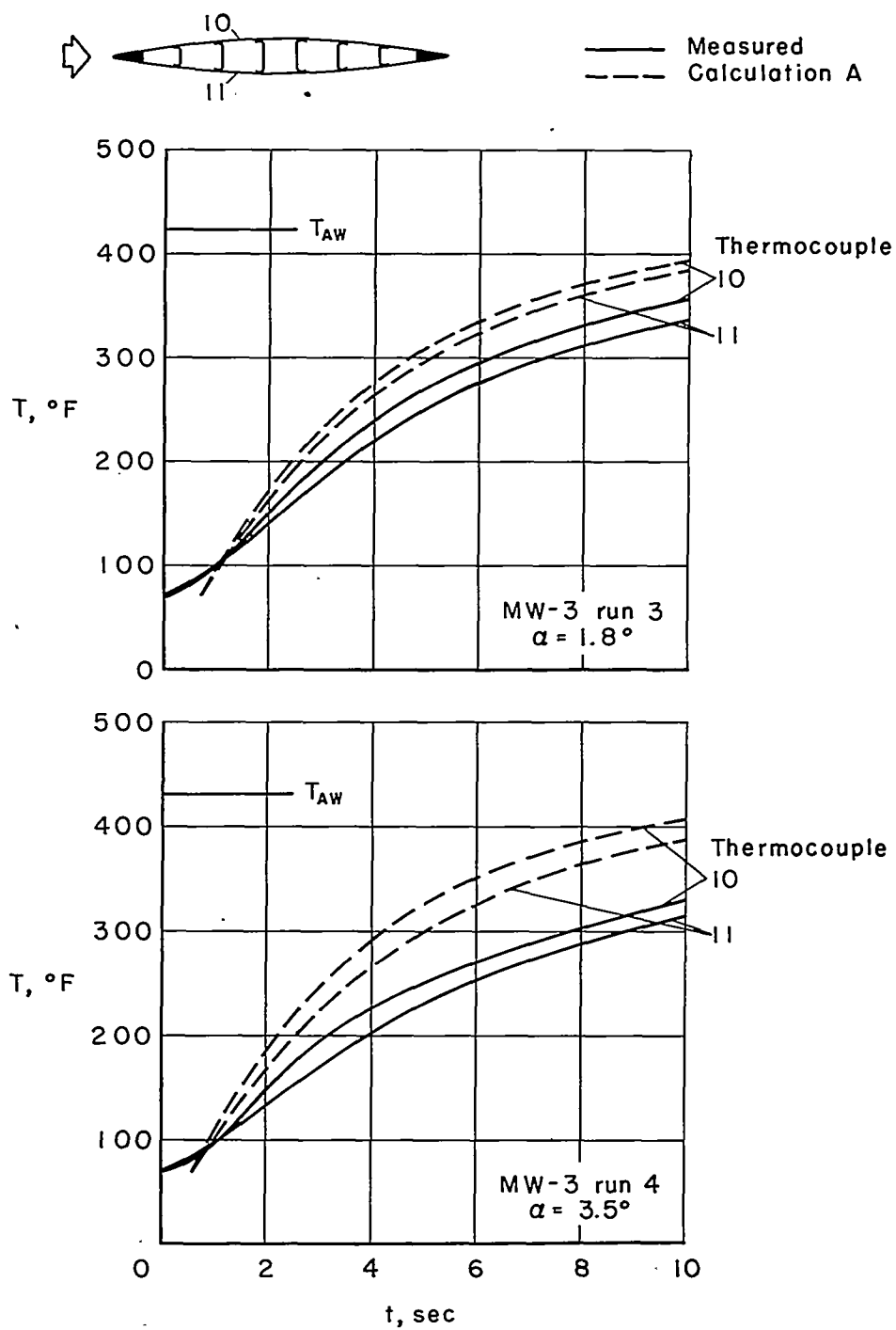
Figure 7.- Concluded..
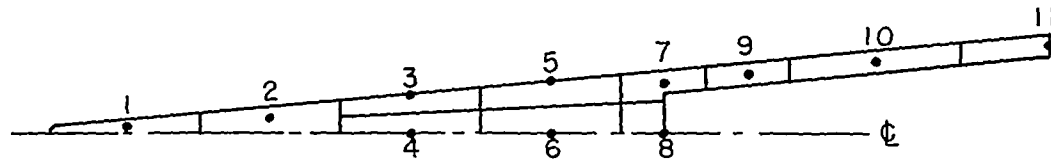
(a) Leading- or trailing-edge section.
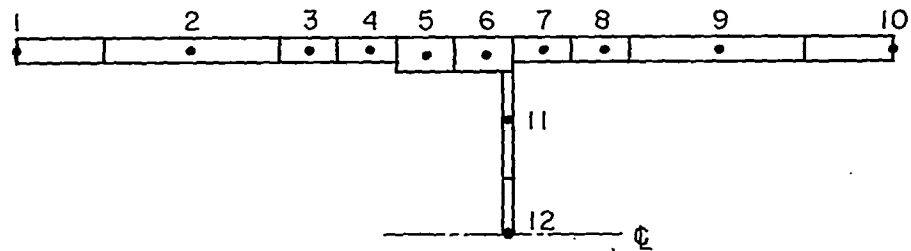
(b) Skin and web combination.

Figure 8.- Subdivision of wing cross section for temperature-distribution calculations.
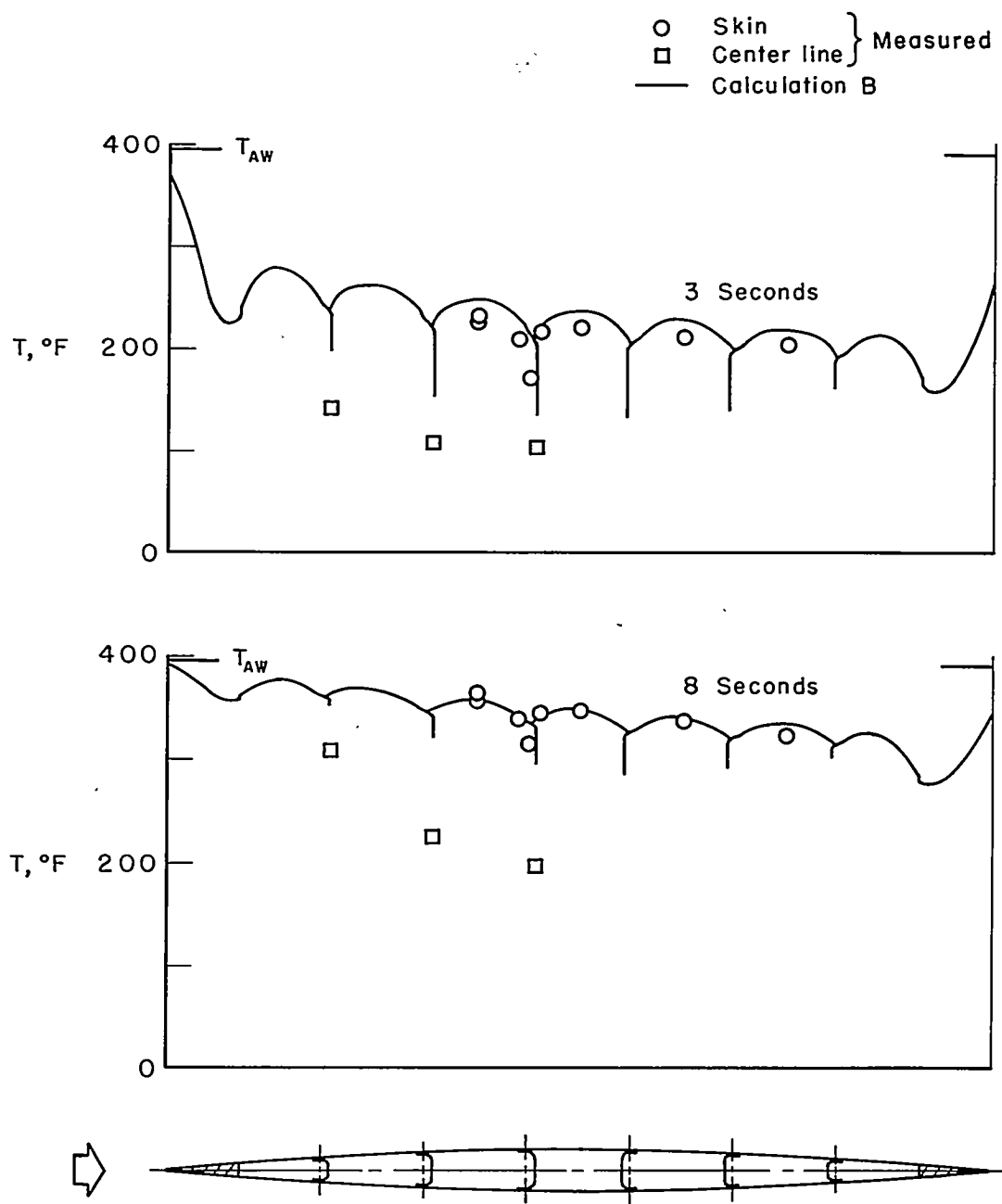
Figure 9.- Temperature distribution of entire cross section of model MW-2.
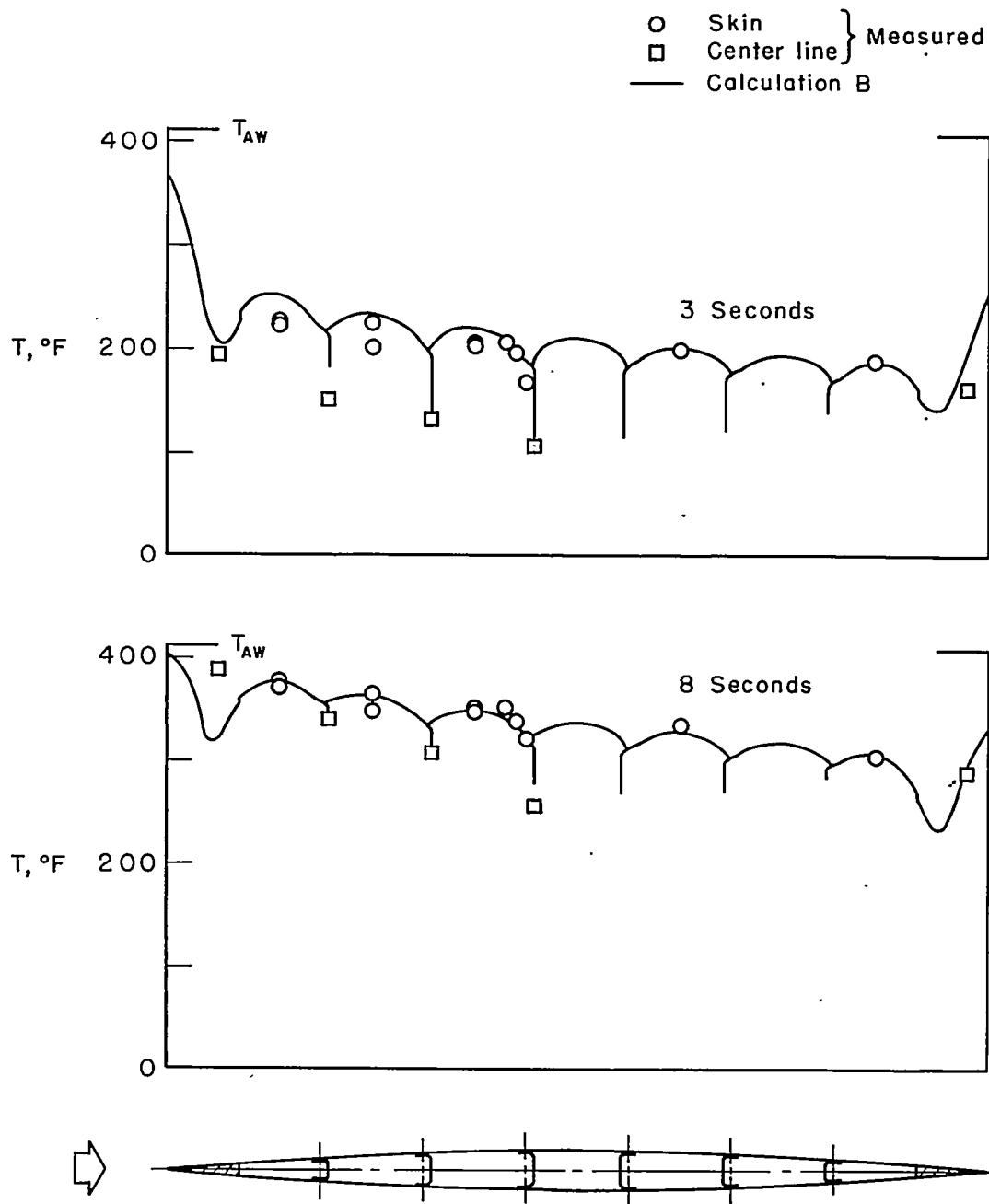
Figure 10.- Temperature distribution of entire cross section of model
MW-3, run 2.
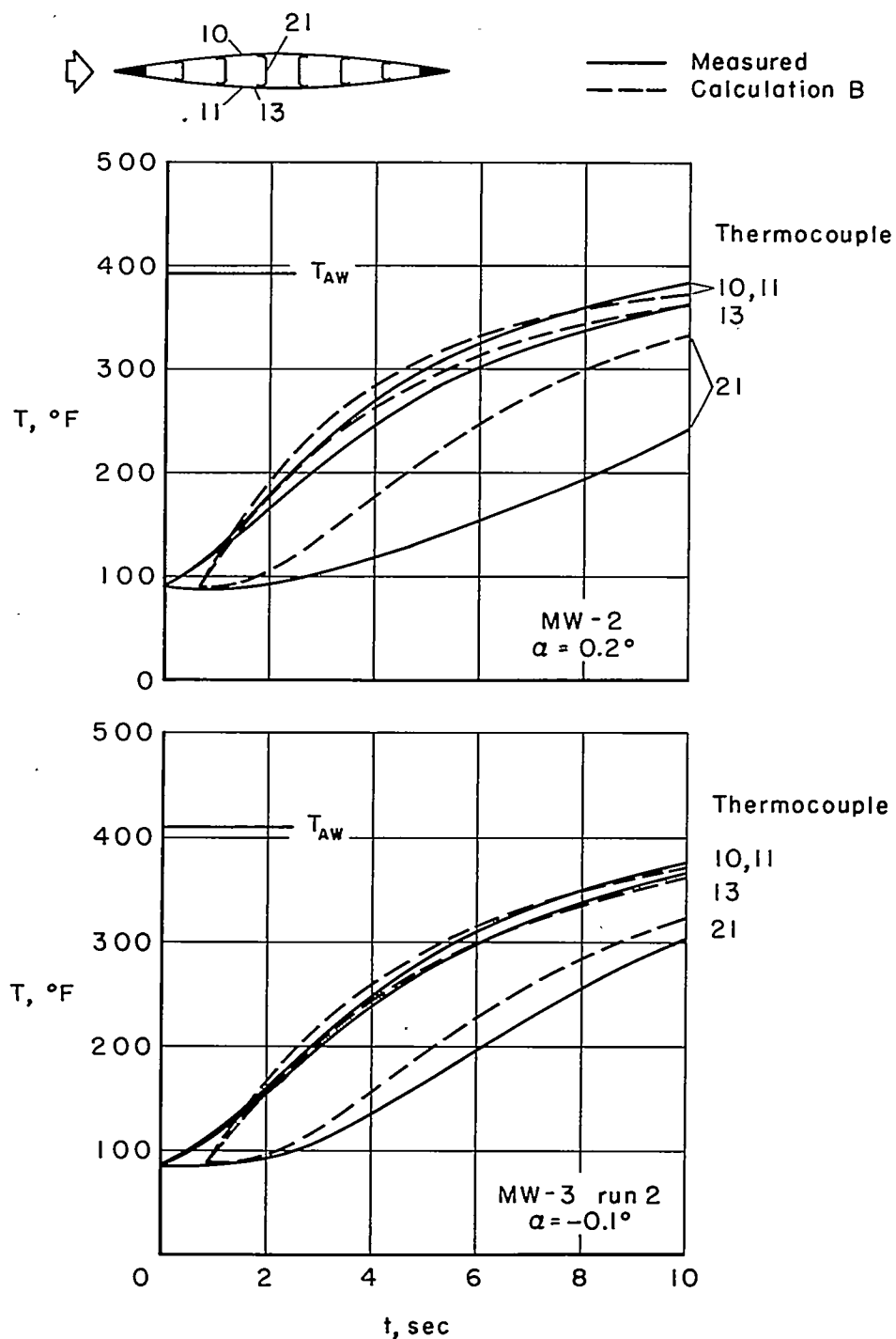
Figure 11.- Comparison of measured and calculated model temperatures.
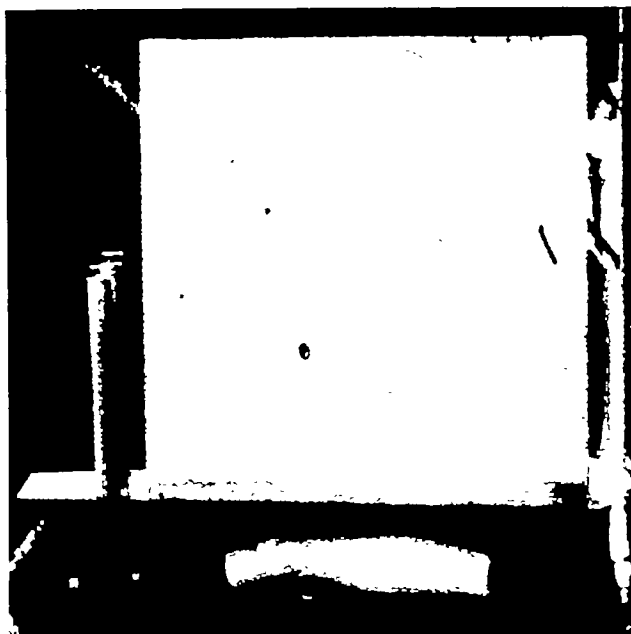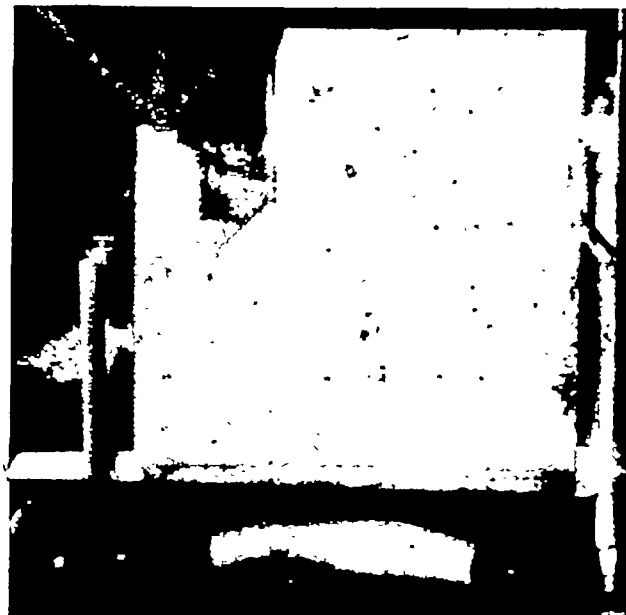
(a)   t = 11.4 seconds.
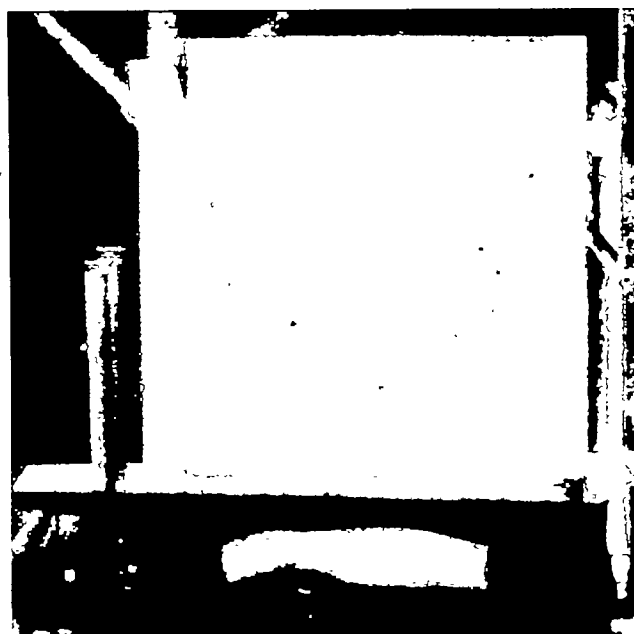
(b)   t = 11.5 seconds.   L-89311
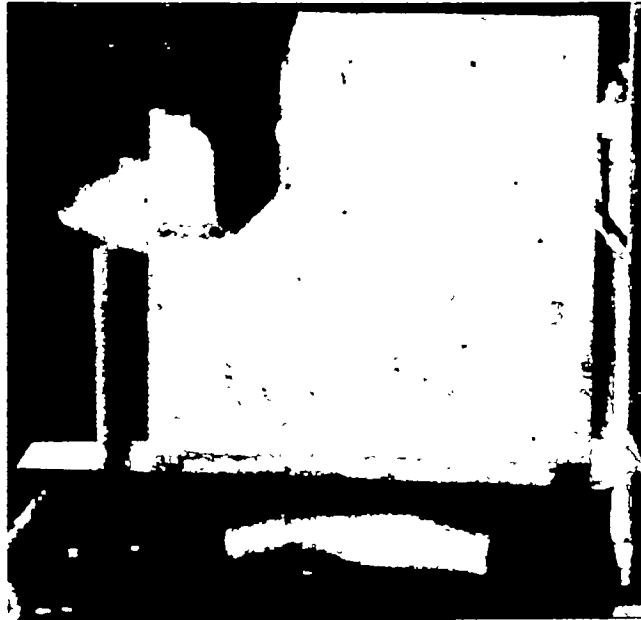
Figure 12.- Progressive failure of model MW-2.

(c) t = 12.3 seconds.

(d) t = 12.3 seconds.   L-89312

Figure 12.- Continued.

(e) t = 12.4 seconds.

(f) t = 13.0 seconds.   L-89313
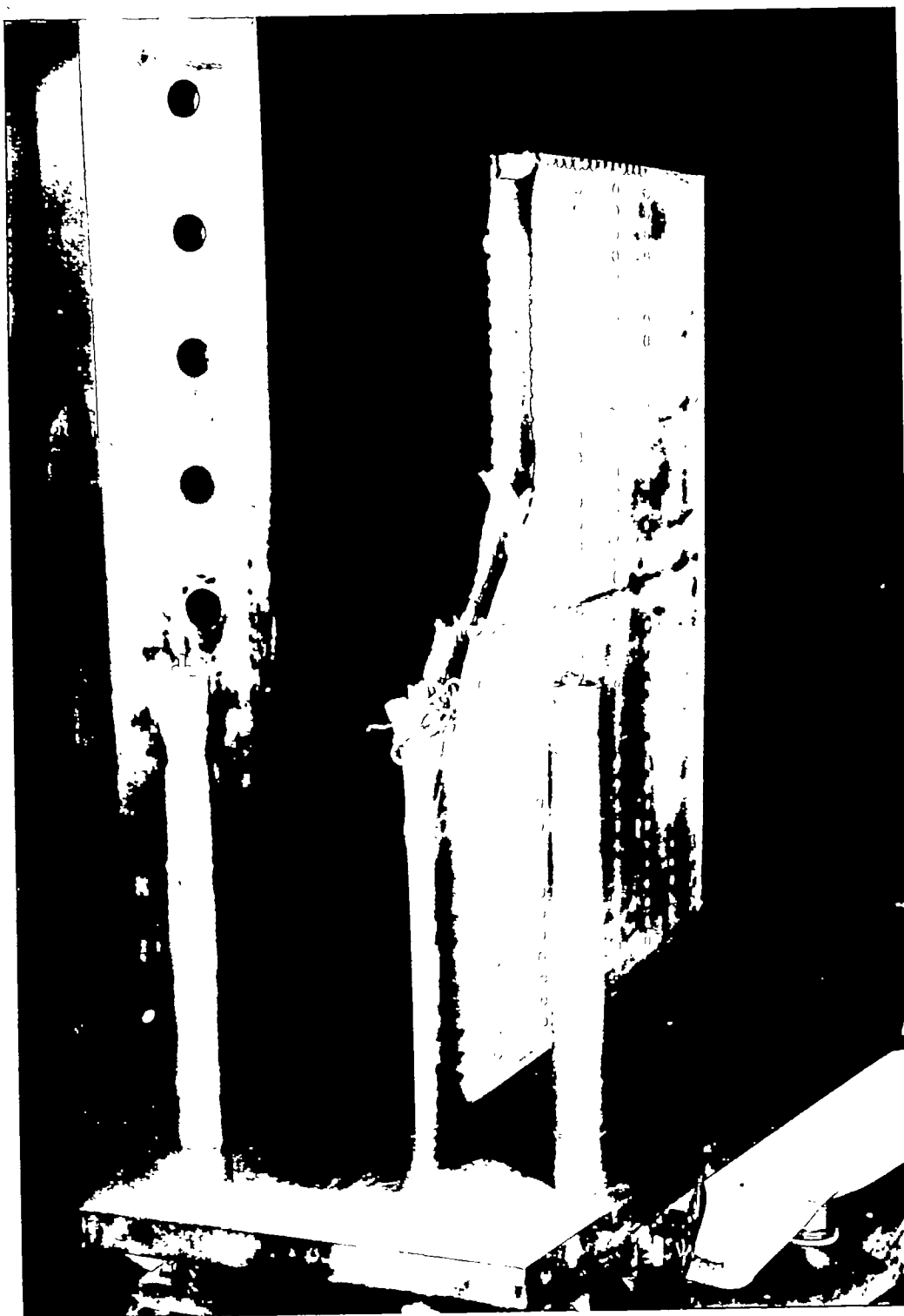
Figure 12.- Concluded.

CONFIDENTIAL

Figure 13.- Model MW-2 after test.

L-77204

Figure 14.- Model MW-3 after failure.   L-77699